J. Fluid Mech. (2005), *vol.* 538, *pp.* 361–376. © 2005 Cambridge University Press
doi:10.1017/S002211200500529X Printed in the United Kingdom

Time singularities in conjugated thermo-fluid-dynamic phenomena

By AMILCARE POZZI AND RENATO TOGNACCINI

Dipartimento di Progettazione Aeronautica, University of Naples "Federico II", Naples, Italy

(Received 10 January 2004 and in revised form 29 March 2005)

The thermo-fluid-dynamic field that arises when an infinite thick plate is impulsively accelerated to a constant speed in a laminar regime is studied, taking into account the coupling of the convection and conduction in the fluid with the conduction in the solid. Two significant cases are discussed depending on the boundary condition imposed on the unwetted side of the plate: constant temperature or adiabatic wall. The work is particularly focused on analysing the singularities arising in the field at the initial time. For this purpose an exact analytical solution of the problem governed by the Navier–Stokes equations with constant properties and by the energy equations in the fluid and in the solid is proposed and discussed. The non-dimensional parameter governing the conjugated effects is shown to be the ratio between the thermal effusivities in the fluid and in the solid. The results have also been extended to the analysis of compressible flows by the Stewartson–Dorodnitsin transformation.

1. Introduction

Exact solutions are very few in the fluid dynamics technical literature, in particular when the boundary conditions are unusual. The specification of the temperature, or of the heat flux, are the typical boundary conditions adopted in the theoretical analysis of the thermo-fluid-dynamic field around a body immersed in a free stream. However, they are not realistic because either the temperature or the heat flux is unknown: on the body surface we can only impose the continuity of these two functions across the solid–fluid interface and we must solve, together with the equations of the fluid motion, the energy equation in the solid; Perelman (1961) named this problem conjugated heat transfer.

The main interest in conjugated effects began with the aerospace industry. New technical applications, such as computer CPU cooling, Cole (1997), or food freezing technology, Moraga & Medina (2000), followed. Recently, a number of papers have studied the influence of conjugated effects on the numerical and experimental analysis of confined turbulent convection, see, among others, Verzicco (2002), Niemela & Sreenivasan (2003), Verzicco (2004).

Due to the complexity of the subject, the conjugated heat transfer effects are often analysed by numerical methods: Tsai, Sheu & Lee (1998), Vynnycky, Kimura & Kanev (1998). Nonetheless an analytic approach, even for very simple geometries, could prove useful in order to manage possible singularities of the solution and to identify how the parameters involved govern the phenomenon. Moreover local asymptotic solutions can be used to quantify these effects quickly for more complex geometries also and, in addition, they are useful tests for experiments.

https://doi.org/10.1017/S002211200500529X Published online by Cambridge University Press

Since the basic works of Luikov, Aleksashenko & Aleksashenko (1971) and Luikov (1974) few analytical results have been presented; a detailed analysis of the literature can be found in Cole (1997). Pozzi & Lupo (1989) discussed a semi-infinite plate in a steady flow. The present case of an infinite thick plate impulsively accelerated from rest in a compressible fluid was studied by Pozzi, Bassano & de Socio (1993). Two conditions were studied consisting of assuming on the unwetted plate side either a constant temperature or an adiabatic condition. A semi-infinite flat plate was considered by Pozzi & Tognaccini (2000, 2001). In these works the authors studied the laminar boundary layer equations coupled with an approximated solution of the temperature field in the solid. These papers showed the appearance of singularities in the solutions at the initial time.

The aim of the present work is to remove the approximation of the temperature field in the solid and to study the importance of these singularities and how they are related to the approximations introduced in the model. Just at the initial time, when the thickness of the plate has the largest influence on the thermo-fluid-dynamic field in the fluid, the approximations in the modelling of the temperature field in the solid could be misleading.

The suddenly accelerated motion from rest to a constant velocity leads to a singular behaviour of the flow because it cannot be described by means of a Taylor expansion. Therefore it is not easy to give a good representation of the phenomenon without an accurate analysis. In the previous work this problem was avoided by a suitable averaging of the quantities of interest. However these approximations are not good for very small values of the time, as the present results will show. Moreover, it is not easy to identify *a priori* the *inlet time*, i.e. the time interval in which the singularity is significant, or the physical parameters governing the phenomenon and the mechanism involved and, hence, how to control it (making these times shorter or longer, for instance). Therefore it is useful to have the exact solution that holds for all times, either small and large.

In addition, we can derive simple expressions for the characteristic times necessary to reach a steady regime, which identify the time interval in which the conjugated effects are significant. These relations can be used, for instance, for verifying the accuracy of measurements of thermal quantities in wind-tunnel simulations of high-speed flows which are usually limited to small times, one of the reasons motivating the studies on conjugated heat transfer in the aerospace research.

Unsteady conjugated effects, such as the ones studied in this work, are also significant in the analysis of turbulent flows, because they can influence the boundary conditions on the wall for the fluctuating thermal field, Schlichting & Gersten (2000). It will be shown that the same non-dimensional parameter controls conjugated effects in both problems.

In the unsteady problem considered here, we study the incompressible, Navier–Stokes equations (laminar flow) for an infinite plate coupled with the *exact* energy equation in the solid. In the range in which the Stewartson–Dorodnitsin transformation is valid, the model can also be applied to the analysis of compressible flows.

We looked for analytical solutions; because of the assumption of an infinite plate (Rayleigh-type flow) both problems, in the fluid and in the solid, are linear, and therefore an approach based on the Laplace transform is appropriate. However the main difficulty found was the definition of a proper procedure for taking into account the coupling of the thermo-fluid-dynamic field in the flow with the temperature field in the solid. This procedure will be presented in the next sections together with the

https://doi.org/10.1017/S002211200500529X Published online by Cambridge University Press

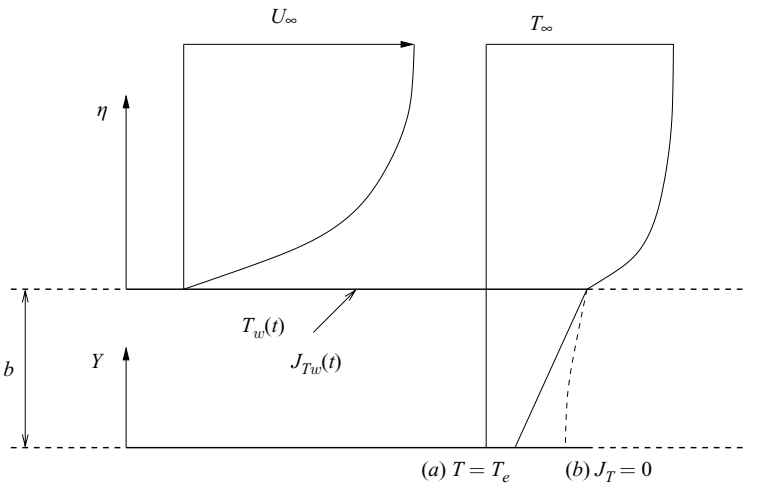


FIGURE 1. Sketch of the impulsive flow arising around an infinite thick plate. The problem depends on the condition imposed on the unwetted plate side: in terms of temperature ($T = T_e$) or heat flux ($J_T = 0$).

extension to the case of compressible flow. The solutions obtained will be discussed and compared with the previous results based on the approximated temperature distribution in the solid. Finally, the results obtained will be summarized in the conclusions together with the most significant simple analytical relations derived in the paper.

2. The infinite thick plate problem

2.1. *Incompressible flow*

We consider an infinite plate (in both directions) of thickness b, wetted by a fluid on one side, which is impulsively accelerated from rest to a constant speed U_∞ at the time $t = 0$. The origin of the spatial coordinate in the fluid, orthogonal to the plate (y) is placed at the solid–fluid interface. The initial temperature field $T(x, y, t)$ is uniform, in both the fluid and the solid: $T(x, y, 0^-) = T_\infty$ (see figure 1). We assume that an incompressible, laminar flow with constant properties (viscosity μ and thermal conductivity λ) arises on the wetted side. Since we are considering an infinite plate, the spatial derivatives in the streamwise direction are vanishing and the Navier–Stokes equations can be further simplified. The boundary conditions for the velocity are matching with the free stream value for $y \to \infty$ and the usual no-slip condition on the plate.

In this case the dynamic field has the well-known solution (Rayleigh flow) $u = \mathrm{erf}[\eta/(2\sqrt{\tau})]$, (White 1974, p. 146), where u is the streamwise velocity component referenced to the free-stream value, erf specifies the error function, $\eta = \sqrt{Re_\infty}\, y/L$ and $\tau = tU_\infty/L$, with Re_∞ the Reynolds number and L a reference length (e.g. $L = b$ or a streamwise reference length).

After defining the non-dimensional temperature $\theta(\tau, \eta) = (T - T_\infty)/T_\infty$ the energy equations in the fluid and in the solid assume the following forms:

$$\frac{\partial \theta}{\partial \tau} - \frac{1}{Pr}\frac{\partial^2 \theta}{\partial \eta^2} = E\left(\frac{\partial u}{\partial \eta}\right)^2, \qquad \frac{\partial \bar{\theta}}{\partial \tau} = t_{\mathrm{fs}}\frac{\partial^2 \bar{\theta}}{\partial Y^2}, \tag{2.1}$$

https://doi.org/10.1017/S002211200500529X Published online by Cambridge University Press

where $\bar{\theta}(\tau, Y)$ is the non-dimensional temperature in the solid, $E = U_\infty^2/(c_p T_\infty)$ (c_p is the specific heat at constant pressure), $t_{\rm fs} = L\alpha_s/(U_\infty b^2)$ is the ratio between the reference times in the fluid and in the solid (α_s is the thermal diffusivity in the solid) and Pr is the Prandtl number. The parameter E is strictly connected with the Eckert number ($Ec = ET_\infty/\Delta T_{ref}$). Y is the spatial coordinate in the solid, orthogonal to the plate, referenced to the plate thickness b and with origin on the unwetted plate side ($Y = 1$ corresponds to $\eta = 0$).

The coupling between the thermal field in the fluid and in the solid is obtained by imposing the continuity of the temperature and of the heat flux at the solid–fluid interface:

$$\theta(\tau, 0) = \bar{\theta}(\tau, 1), \qquad p\frac{\partial\theta}{\partial\eta}(\tau, 0) = \frac{\partial\bar{\theta}}{\partial Y}(\tau, 1), \tag{2.2}$$

where $p = (b/L)(\lambda_\infty/\lambda_s)\sqrt{Re_\infty}$ (λ_s is the thermal conductivity in the solid) and is directly related to the Brun number introduced by Luikov (1974) (${\rm Br} = p\sqrt{Pr}$); p and $t_{\rm fs}$ are the additional parameters ruling the conjugated heat transfer phenomena. We shall show later that a single parameter Λ can describe the conjugated effects if the time is referenced to the reference time in the solid. However this choice makes the analysis of the results more difficult.

Two cases are studied here, depending on the condition imposed on the unwetted side of the plate:

(*a*) *isothermal case*, the temperature is kept at a constant value $\bar{\theta}(\tau, 0) = \theta_e$;

(*b*) *adiabatic case*, the heat flux is zero, $\partial\bar{\theta}/\partial Y(\tau, 0) = 0$.

Case (*b*) also provides the solution of the important problem consisting of a symmetrical flow around a thick plate (with thickness $2b$) wetted by the fluid on both sides.

2.2. *Compressible flow*

As discussed in detail by Van Dyke (1952) and Hanin (1960) the compressibility complicates the problem of the thermal field in the Rayleigh flow. However, the same mathematical model also governs the problem in the case of compressible flow by introducing some approximations. In the case of a boundary layer flow, the Stewartson–Dorodnitsin transformation (also called Dorodnitsin–Howarth, Schlichting & Gersten 2000, p. 246) makes it possible to decouple the energy equation from the continuity and momentum ones. Assuming $\mu/\mu_\infty = \lambda/\lambda_\infty = \rho_\infty/\rho = T/T_\infty$ (ρ is the fluid density), this transformation is given by

$$\eta = \frac{\sqrt{Re_\infty}}{L}\int_0^y \frac{\rho}{\rho_\infty}\,{\rm d}y, \qquad \tau = \frac{tU_\infty}{L}. \tag{2.3}$$

The solution of the dynamic field is again the error function and the energy equations (2.1) are exactly recovered with $E = (\gamma - 1)M_\infty^2$, where γ is the ratio between the specific heats and M_∞ is the free-stream Mach number.

The Stewartson–Dorodnitsin transformation assumes a linear variation with temperature of the fluid properties μ and λ. However it can also be applied by considering a suitable linearization of the more general Sutherland law as indicated in Schlichting & Gersten 2000, p. 243), which allows one to write $\mu/\mu_\infty = \lambda/\lambda_\infty = k_\mu T/T_\infty$. In this case it is only necessary to substitute in equations (2.3) a modified Reynolds number $\bar{R}e = Re_\infty/k_\mu$.

Therefore in the following, the results proposed can be used to discuss both the *exact* incompressible problem or the *approximated* compressible case; in the latter, the

https://doi.org/10.1017/S002211200500529X Published online by Cambridge University Press

Stewartson–Dorodnitsin inverse transformation is only required to obtain the results in the physical space.

2.3. *Previous results*

In Pozzi *et al.* (1993) a solution of this problem was proposed. However, the thermal field in the solid was approximated by linear (in the isothermal case) and by parabolic (in the adiabatic case) distributions. In this way, after integration of the energy equation with respect to Y it was possible to derive a coupling condition written in terms of variables of the fluid field only.

An interesting result of the analytical solutions obtained in that work was the particular behaviour of the solution near the solid–fluid interface at the initial time: in the isothermal case at $\tau = 0$ the interface temperature was continuous; on the contrary, in the adiabatic case, a jump in the temperature was found.

3. The solution in the transformed variables

3.1. *The solution for the fluid*

A particular integral of the energy equation in the fluid can be found by looking for self-similar solutions: by means of the similarity variable $\zeta_T = \sqrt{Pr}\eta/(2\sqrt{\tau})$ it is possible to obtain

$$\theta_p(\zeta_T) = E\left[\frac{2}{\pi}\frac{\arctan(K)}{K} - \frac{2}{\sqrt{\pi}}\int_0^{\zeta_T} f(\xi)\,\mathrm{d}\xi + \frac{1}{K}\mathrm{erfc}\zeta_T\mathrm{erf}(K\zeta_T)\right], \tag{3.1}$$

where erfc specifies the complementary error function, $K^2 = 2/Pr - 1$, and, in the case of a fluid with $Pr < 2$:

$$f(\xi) = \mathrm{e}^{-(K\xi)^2}\mathrm{erfc}(\xi). \tag{3.2}$$

Useful properties of this solution are

$$\theta_p(\tau, 0) = E\frac{2}{\pi}\frac{\arctan(K)}{K}, \quad \theta_p(0, \eta) = 0, \quad \frac{\partial\theta_p}{\partial\eta}(\tau, 0) = 0, \quad \frac{\partial\theta_p}{\partial\tau}(0, 0) = 0. \tag{3.3}$$

θ_p is the solution of the temperature field in the case of Rayleigh flow over a plate with infinitely small thickness ($b = 0$) and an adiabatic wall. $\theta_{aw} = 2E\arctan K/(\pi K)$ is the adiabatic wall temperature. Pozzi & Tognaccini (2004) discussed in detail this particular solution corresponding to the non-conjugated problem in the fluid; they also provided analytical expressions for the recovery factor in the adiabatic case and for the Nusselt number in the isothermal case. In the same reference, the solution for $Pr > 2$ is also discussed (in this case K is imaginary, but equation (3.1) is still valid).

Let $\Theta(s, \eta)$ be the Laplace transform of $\theta(\tau, \eta)$ with respect to τ, then the homogeneous equation associated with the energy equation for the fluid in transformed variables reduces to

$$\frac{\partial^2\Theta}{\partial\eta^2} - sPr\Theta = 0, \tag{3.4}$$

which is still homogeneous because $\theta(0^+, \eta) = 0$ due to the boundary conditions. Therefore, considering that θ vanishes as $\eta \to \infty$, the transformed solution for the fluid is

$$\Theta(s, \eta) = \Theta_{h_w}(s)\mathrm{e}^{-\sqrt{Pr}\sqrt{s}\eta} + \Theta_p(s, \eta), \tag{3.5}$$

https://doi.org/10.1017/S002211200500529X Published online by Cambridge University Press

where $\Theta_p(s,\eta)$ is the Laplace transform of equation (3.1). In particular, at the solid–fluid interface:

$$\Theta_w(s)=\Theta_{h_w}(s)+\frac{\theta_{aw}}{s},\qquad \left(\frac{\partial\Theta}{\partial\eta}\right)_w(s)=\sqrt{sPr}\left[\frac{\theta_{aw}}{s}-\Theta_w(s)\right]. \tag{3.6}$$

These relations show that, at the solid–fluid interface, the temperature gradient in the fluid can be expressed in terms of the unknown transformed temperature $\Theta_w(s)$.

It is now necessary to find the temperature distribution in the solid and, then, to couple the thermal fields in the fluid and in the solid.

3.2. *The solution for the solid*

Denoting by $\bar{\Theta}(s,Y)$ the Laplace transform of $\bar{\theta}(\tau,Y)$ we have from the second of equations (2.1)

$$\frac{\partial^2\bar{\Theta}}{\partial Y^2}-\frac{s}{t_{\rm fs}}\bar{\Theta}=0. \tag{3.7}$$

This equation is homogeneous since $\bar{\theta}(0^+,Y)=0$ (at the initial time the temperature in the solid is uniform and equals T_∞).

When a constant temperature θ_e is imposed at $Y=0$ (isothermal case), the solution is

$$\bar{\Theta}(s,Y)=\frac{1}{\sinh\left(\sqrt{s/t_{\rm fs}}\right)}\left\{\frac{\theta_e}{s}\sinh\left[\sqrt{\frac{s}{t_{\rm fs}}}(1-Y)\right]+\bar{\Theta}_w(s)\sinh\left(\sqrt{\frac{s}{t_{\rm fs}}}Y\right)\right\}, \tag{3.8}$$

where $\bar{\Theta}_w(s)$ is the transformed temperature at the solid–fluid interface. In particular the transformed temperature gradient at the solid–fluid interface is

$$\left(\frac{\partial\bar{\Theta}}{\partial Y}\right)_w=\sqrt{\frac{s}{t_{\rm fs}}}\left[\frac{\bar{\Theta}_w(s)}{\tanh\left(\sqrt{s/t_{\rm fs}}\right)}-\frac{\theta_e}{s}\frac{1}{\sinh\left(\sqrt{s/t_{\rm fs}}\right)}\right]. \tag{3.9}$$

Again, at the solid–fluid interface, the transformed temperature gradient has been expressed in terms of the transformed temperature.

In the adiabatic case $\partial\bar{\theta}/\partial Y(\tau,0)=0$. The solution of equation (3.7) is

$$\bar{\Theta}(s,Y)=\bar{\Theta}_w(s)\frac{\cosh\left(\sqrt{s/t_{\rm fs}}Y\right)}{\cosh\left(\sqrt{s/t_{\rm fs}}\right)} \tag{3.10}$$

and, at the solid–fluid interface:

$$\left(\frac{\partial\bar{\Theta}}{\partial Y}\right)_w=\bar{\Theta}_w(s)\sqrt{\frac{s}{t_{\rm fs}}}\tanh\left(\sqrt{\frac{s}{t_{\rm fs}}}\right). \tag{3.11}$$

In the fluid and in the solid the only unknowns are $\Theta_w(s)$ and $\bar{\Theta}_w(s)$ respectively.

3.3. *Coupling of the solid–fluid thermal field*

The mathematical model is closed by imposing the coupling conditions (2.2) in terms of the transformed variables:

$$\Theta_w(s)=\bar{\Theta}_w(s),\qquad p\left(\frac{\partial\Theta}{\partial\eta}\right)_w(s)=\left(\frac{\partial\bar{\Theta}}{\partial Y}\right)_w(s). \tag{3.12}$$

The substitution of the expressions for $(\partial\Theta/\partial\eta)_w$ and $(\partial\bar{\Theta}/\partial Y)_w$ in equations (3.12) provides the transformed interface temperature for both the isothermal and adiabatic case:

https://doi.org/10.1017/S002211200500529X Published online by Cambridge University Press

isothermal case

$$\Theta_w(s) = \frac{1}{s}\frac{\theta_{aw}\Lambda e^{\sigma} - \Lambda e^{-\sigma} + 2\theta_e}{(1+\Lambda)e^{\sigma} + (1-\Lambda)e^{-\sigma}}, \tag{3.13a}$$

adiabatic case

$$\Theta_w(s) = \frac{\theta_{aw}\Lambda}{s}\frac{e^{\sigma} + e^{-\sigma}}{(1+\Lambda)e^{\sigma} - (1-\Lambda)e^{-\sigma}}, \tag{3.13b}$$

where $\sigma = \sqrt{s/t_{fs}}$ and $\Lambda = p\sqrt{t_{fs}}\sqrt{Pr}$.

The problem is solved once $\Theta(s,\eta)$ and $\bar{\Theta}(s,Y)$ are inversely transformed into the physical variables $\theta(\tau,\eta)$ and $\bar{\theta}(\tau,Y)$.

4. The temperature at the solid–fluid interface

The inverse transformation can be obtained more easily after performing a series expansion of equations (3.13). The application of some properties of the binomial series, see Abramowitz & Stegun (1965, p. 15), makes it possible to write

$$(1 + Ae^{-2\sigma})^{-1} = \sum_{n=0}^{\infty}(-A)^n e^{-2n\sigma}, \qquad (1 - Ae^{-2\sigma})^{-1} = \sum_{n=0}^{\infty} A^n e^{-2n\sigma}, \tag{4.1}$$

where $A = (1-\Lambda)/(1+\Lambda)$. These series are absolutely convergent for $|Ae^{-2\sigma}| < 1$, a condition always satisfied ($\Lambda > 0$ is required). Substituting the first expression into equation (3.13*a*) and the second into equation (3.13*b*), we obtain

isothermal case

$$\Theta_w(s) = \frac{1}{s}\left\{\theta_{w0} + \kappa\left[\theta_e\sum_{n=0}^{\infty}(-A)^n e^{-(2n+1)\sigma} - \theta_{w0}\sum_{n=0}^{\infty}(-A)^n e^{-2(n+1)\sigma}\right]\right\}, \tag{4.2a}$$

adiabatic case

$$\Theta_w(s) = \frac{\theta_{w0}}{s}\sum_{n=0}^{\infty} A^n\left[e^{-2n\sigma} + e^{-(2n+1)\sigma}\right], \tag{4.2b}$$

where $\theta_{w0} = \theta_{aw}\Lambda/(1+\Lambda)$ and $\kappa = 2/(1+\Lambda)$.

The inverse transform of these relations, i.e. the physical temperature at the solid–fluid interface, can be obtained in analytical form, see Erdélyi (1954):

isothermal case

$$\theta_w(\tau) = \theta_{w0}\left[1 - \kappa\sum_{n=0}^{\infty}(-A)^n \operatorname{erfc}\left(\frac{n+1}{\sqrt{t_{fs}\tau}}\right)\right] + \kappa\theta_e\sum_{n=0}^{\infty}(-A)^n \operatorname{erfc}\left(\frac{2n+1}{2\sqrt{t_{fs}\tau}}\right), \tag{4.3a}$$

adiabatic case

$$\theta_w(\tau) = \theta_{w0}\left[1 + \kappa\sum_{n=0}^{\infty} A^n \operatorname{erfc}\left(\frac{n+1}{\sqrt{t_{fs}\tau}}\right)\right]. \tag{4.3b}$$

The analysis of these relations shows that both solutions are characterized at the initial time, when the plate is impulsively accelerated, by a jump of the interface temperature (θ_{w0}), which is the same for both cases. It depends on the adiabatic wall temperature (θ_{aw}) and on Λ. For $\Lambda \to 0$ $\theta_{w0} \to 0$, while for $\Lambda \to \infty$ $\theta_{w0} \to \theta_{aw}$. This behaviour is different from that predicted in Pozzi *et al.* (1993), where the conjugated effects were taken into account by an approximating procedure. In the previous work the temperature was found to be continuous at the initial time for the isothermal

https://doi.org/10.1017/S002211200500529X Published online by Cambridge University Press

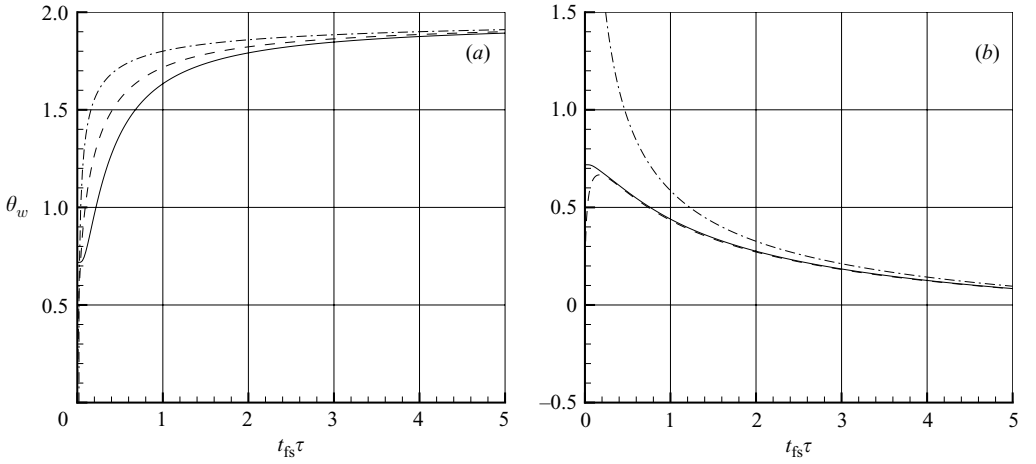


FIGURE 2. Temperature at the solid–fluid interface against time in the isothermal case. $E = 3.6$, $Pr = 0.7$, $\Lambda = 0.8367$. —, present solution (relations (4.3*a*)); ——, Pozzi *et al.* (1993); —·—, asymptotic formula (4.4*a*). (*a*) $\theta_e = 2$ (heating); (*b*) $\theta_e = -0.3$ (cooling).

case. On the contrary, a temperature jump was found in the adiabatic case; however this discontinuity was independent of the coupling parameter Λ, and was given by $\theta_w(0^+) = \theta_{aw}$.

If the time variable is referenced to the reference time in the solid $\bar{\tau} = t_{fs}\tau$, the only parameter related to the conjugated phenomenon and influencing the non-dimensional temperature at the solid–fluid interface is $\Lambda = p\sqrt{t_{fs}}\sqrt{Pr}$ (and, obviously, θ_e in the isothermal case). Therefore Λ is the only parameter characterizing the conjugated effects when the time is referenced to the characteristic time in the solid (the adopted time scale is important because defines the time interval in which the conjugated effects are significant). Λ has an interesting physical meaning: $\Lambda = b/L\ E_R$, where E_R is the ratio between $e_f = \sqrt{\rho_\infty c_p \lambda_\infty}$ and $e_s = \sqrt{\rho_s c_s \lambda_s}$ which are respectively the thermal effusivity in the fluid and in the solid (ρ_s and c_s are the density and the specific heat of the solid). The thermal effusivity characterizes the ability to exchange thermal energy with the surroundings. By choosing $L = b$, we obtain that the conjugated effects are ruled by $\Lambda = E_R$, the effusivity ratio. It is the same kind of phenomenon shown by Schlichting & Gersten (2000, p. 507). They suggested that 'a constant temperature assigned at the wall is a physically correct boundary condition for the energy equation in a turbulent flow when $\rho_s c_s \lambda_s$ is very large'.

The interface temperatures are plotted against $t_{fs}\tau$ in figure 2 for the isothermal case and in figure 3 for the adiabatic case, with the conditions $E = 3.6$, $Pr = 0.7$, $\Lambda = 0.8367$. The condition $E = 3.6$ is equivalent to $M_\infty = 3$ in air. The series in equations (4.3) are quickly converging; however 40 terms in the summations have been used in the plots. The previous solutions of Pozzi *et al.* (1993) are also plotted. Despite the different behaviour at the initial time, agreement with the previous results is recovered as time grows. Figure 2(*a*) shows a case in which the plate is heated ($\theta_e > 0$), while in figure 2(*b*) the plate is cooled ($\theta_e < 0$). Although the error due to the approximations of the previous solution depends on E_R and $|\theta_e|$, we systematically noted smaller errors in the cooling case, which can be explained by the analysis of the thermal field in the solid that will follow in one of the next sections. In the adiabatic case in figure 3 the usual asymptotic behaviour, not shown

https://doi.org/10.1017/S002211200500529X Published online by Cambridge University Press

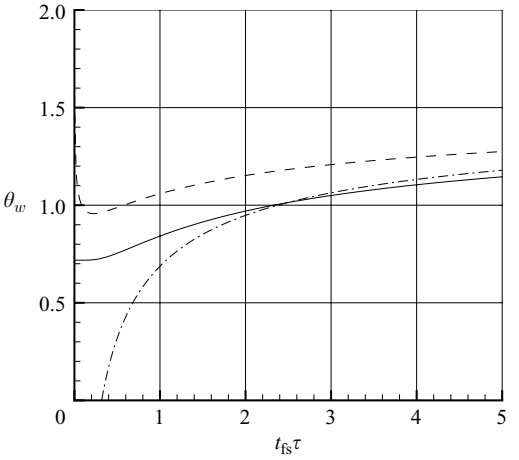


FIGURE 3. Temperature at the solid–fluid interface against time in the adiabatic case. $E = 3.6$, $Pr = 0.7$, $\Lambda = 0.8367$. —, present solution (relations (4.3*b*)); ——, Pozzi *et al.* (1993); —·—, asymptotic formula (4.4*b*).

in the figure, is only recovered for very large time values. Since E_R is small in many practical applications (air–metal for instance) the temperature jump θ_{w0} can be small and the error of the previous solution can be large, especially in the adiabatic case.

The steady solution is characterized by $\theta_w = \theta_e$, in the isothermal case, and by $\theta_w = \theta_{aw}$ (the adiabatic wall temperature) in the adiabatic case which allows thermal equilibrium to be reached in the solid. These results follow from equations (4.3), taking into account equations (4.1) that give for $\tau \to \infty$ ($\sigma \to 0$) $\sum_{n=0}^{\infty}(\pm A)^n = 1/(1 \mp \Lambda)$.

The leading terms in the summations of relations (4.3) provide the local solution of θ_w for $\tau \to 0$. A more convenient way to perform the local and the asymptotic analysis is in the transformed space, as briefly discussed in the Appendix. The asymptotic behaviour ($\tau \to \infty$), also plotted in the figures, is given by

isothermal case

$$\theta_w(\tau) \approx \theta_e + (\theta_{aw} - \theta_e)\frac{\Lambda}{\pi\sqrt{t_{fs}\tau}}, \tag{4.4a}$$

adiabatic case

$$\theta_w(\tau) \approx \theta_{aw}\left(1 - \frac{1}{\pi\Lambda\sqrt{t_{fs}\tau}}\right). \tag{4.4b}$$

The non-dimensional time necessary to reach the steady state can be easily quantified by these relations.

In figure 4 the effects of the coupling parameter Λ on the interface temperature are shown. During the transitional regime, in the isothermal case, for $\theta_{aw} > \theta_e$, a peak value of the interface temperature is reached, with the corresponding time depending on Λ.

This figure also shows when conjugated effects are significant (with time referenced to properties of the solid). In particular, in the isothermal case, they would be negligible in the case of a sudden jump of the interface temperature to $\theta_w = \theta_e$, which is obtained for $\Lambda \to 0$. On the contrary, in the adiabatic case, a sudden jump of the interface temperature to the adiabatic wall temperature (characterizing the absence

https://doi.org/10.1017/S002211200500529X Published online by Cambridge University Press

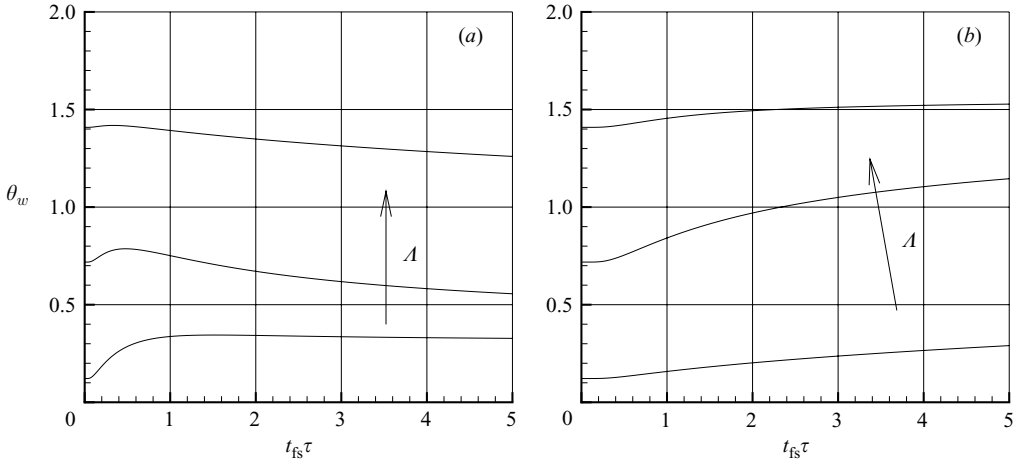


FIGURE 4. Temperature at the solid–fluid interface against time: (*a*) isothermal case; (*b*) adiabatic case. $E = 3.6$, $Pr = 0.7$, $\Lambda = 0.0837, 0.837, 8.37$ ($\theta_e = 0.3$ in the isothermal case).

of conjugated effects) is obtained for $\Lambda \to \infty$. A noteworthy case is obtained when $\Lambda = 1$, i.e. thermal effusivities in the fluid and in the solid are equal: in this case $A = 0$ and only the leading terms in the summations of equations (4.3) are different from zero.

By referencing the heat flux at the solid–fluid interface to dimensional parameters of the solid we introduce the Nusselt number $Nu_s = (\partial\bar{\theta}/\partial Y)_w = p(\partial\theta/\partial\eta)_w$, the last equality deriving from the coupling conditions (2.2). Nu_s can be obtained by performing the inverse transform of the second equation of (3.6):

isothermal case

$$Nu_s(t_{fs}\tau) = \frac{\Lambda}{\sqrt{\pi}\sqrt{t_{fs}\tau}}\left[\theta_{aw} - \theta_{w0} + \kappa\theta_{w0}\sum_{n=0}^{\infty}(-A)^n \mathrm{e}^{-(n+1)^2/(t_{fs}\tau)} - \kappa\theta_e\sum_{n=0}^{\infty}(-A)^n \mathrm{e}^{-(2n+1)^2/(4t_{fs}\tau)}\right], \quad (4.5a)$$

adiabatic case

$$Nu_s(t_{fs}\tau) = \frac{\Lambda}{\sqrt{\pi}\sqrt{t_{fs}\tau}}\left[\theta_{aw} - \theta_{w0} - \kappa\theta_{w0}\sum_{n=0}^{\infty}A^n \mathrm{e}^{-(n+1)^2/(t_{fs}\tau)}\right]. \quad (4.5b)$$

In both cases the heat flux is infinite for $\tau \to 0$ with the local behaviour

$$Nu_s(t_{fs}\tau) \approx \frac{\Lambda}{\sqrt{\pi}\sqrt{t_{fs}\tau}}(\theta_{aw} - \theta_{w0}) = \frac{\Lambda}{1+\Lambda}\frac{\theta_{aw}}{\sqrt{\pi}\sqrt{t_{fs}\tau}}. \quad (4.6)$$

This relation and the local analysis of equation (4.3) show that for $\tau \to 0$ the temperature and the heat flux at the solid–fluid interface are the same in both the isothermal and adiabatic case; therefore they do not depend on the condition imposed on the unwetted side of the plate. Since $\theta_{aw} - \theta_{w0} > 0$, at the very initial time the fluid is always heating the plate. For large time values the heat flux is vanishing in both cases; however, in the isothermal case, the plate will heat the fluid if $\theta_e > \theta_{aw}$

https://doi.org/10.1017/S002211200500529X Published online by Cambridge University Press

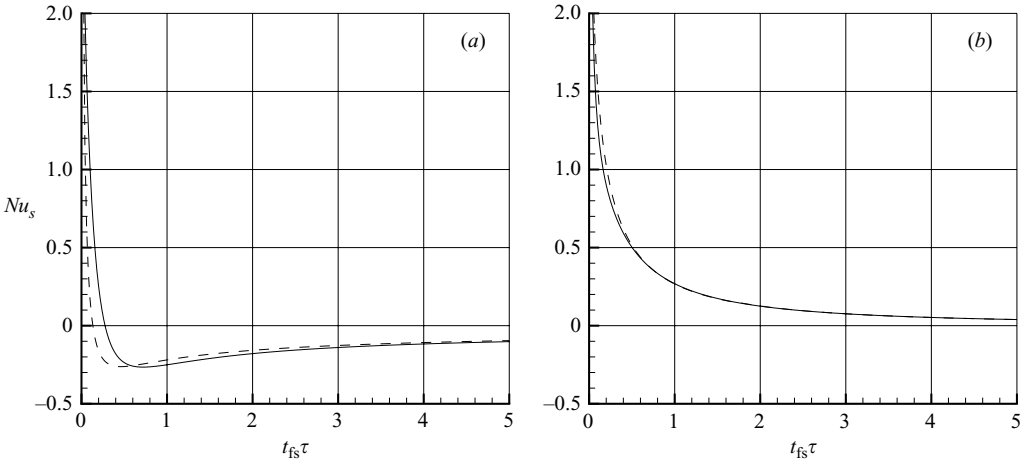


FIGURE 5. Heat flux at the solid–fluid interface against time: (*a*) isothermal case; (*b*) adiabatic case. —, present solution; ——, Pozzi *et al.* (1993). $E = 3.6$, $Pr = 0.7$, $\Lambda = 0.837$ ($\theta_e = 2$ in the isothermal case).

which implies the existence of a time value characterized by zero heat flux. These results, compared with Pozzi *et al.* (1993), are shown in figure 5.

The influence of the coupling parameter Λ on the heat flux needs further analysis. The asymptotic analysis for $\tau \to \infty$ provides

isothermal case

$$Nu_s(t_{fs}\tau) = \frac{\Lambda}{\sqrt{\pi}\sqrt{t_{fs}\tau}}(\theta_{aw} - \theta_e), \tag{4.7a}$$

adiabatic case

$$Nu_s(t_{fs}\tau) = \frac{\theta_{aw}}{2\sqrt{\pi}(t_{fs}\tau)^{3/2}}. \tag{4.7b}$$

The asymptotic stage of Nu_s does not depend on the coupling parameter Λ in the adiabatic case. This relation can provide an alternative definition of the characteristic time for which the conjugated effects are negligible. However in the definition of Nu_s a scale defined by the solid properties appears. In terms of parameters of the fluid the alternative definition of the Nusselt number would be $Nu_f = \sqrt{Re_\infty Pr t_{fs}} Nu_s/\Lambda$. Therefore, in terms of fluid properties, the asymptotic heat flux depends on Λ, although the parameter t_{fs} also appears (which is true for any quantity expressed in terms of fluid properties).

5. The temperature distribution in the fluid

$\theta_p(\zeta_T)$ is already known in the physical space, therefore the determination of the temperature field in the fluid only requires the inverse transform of $\bar{\Theta}(s, \eta)$ (relation (3.5)). This operation does not cause additional difficulties once the series expressions of $\Theta_w(s)$ are known (equations (4.2)) and taking into account that $\Theta_{h_w}(s) = \Theta_w(s) - \theta_{aw}/s$, due to equations (3.6) and (3.3). In particular we obtain

https://doi.org/10.1017/S002211200500529X Published online by Cambridge University Press

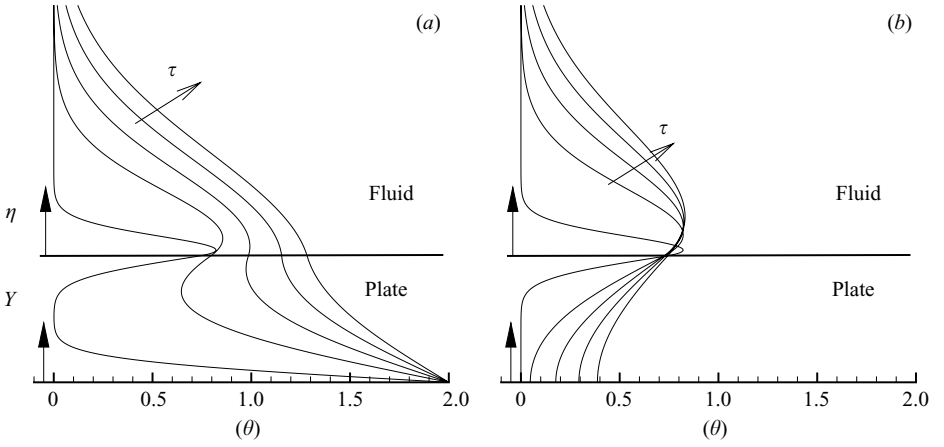


FIGURE 6. Temperature distribution in the fluid and in the solid for different time values: (*a*) isothermal case; (*b*) adiabatic case. $E=3.6$, $Pr=0.7$, $\Lambda=0.837$, $t_{\rm fs}=1$, $\tau=0.01$, 0.11, 0.21, 0.31, 0.41. $\theta_e=2$ in the isothermal case.

isothermal case

$$\theta(\tau,\eta)=\theta_i(\zeta_T)-\kappa\theta_{w0}\sum_{n=0}^{\infty}(-A)^n\mathrm{erfc}\left(\frac{n+1}{\sqrt{t_{\rm fs}\tau}}+\zeta_T\right)+\kappa\theta_e\sum_{n=0}^{\infty}(-A)^n\mathrm{erfc}\left(\frac{2n+1}{2\sqrt{t_{\rm fs}\tau}}+\zeta_T\right), \tag{5.1a}$$

adiabatic case

$$\theta(\tau,\eta)=\theta_i(\zeta_T)+\kappa\theta_{w0}\sum_{n=0}^{\infty}A^n\mathrm{erfc}\left(\frac{n+1}{\sqrt{t_{\rm fs}\tau}}+\zeta_T\right), \tag{5.1b}$$

where

$$\theta_i(\zeta_T)=(\theta_{w0}-\theta_{aw})\mathrm{erfc}\zeta_T+\theta_p(\zeta_T). \tag{5.2}$$

Both solutions are made up of a self-similar term $\theta_i(\zeta_T)$ and the remaining part which is not self-similar. The self-similar part $\theta_i(\zeta_T)$ is the leading term for $\tau\to0$ in both cases. Therefore, for small time values, the solution in the fluid is self-similar and independent of the condition imposed on the unwetted side of the plate. It is interesting to note that, in the isothermal case with $\theta_e>\theta_{aw}$, at the very initial time, the plate is heated from both sides. The time evolution of the temperature distribution in the fluid is plotted in figure 6 for both the isothermal and adiabatic cases and for the same flow conditions as the previous figures. These profiles are also valid in the case of compressible flow by the Stewartson–Dorodnitsin transformation. However the temperature distribution in the fluid influences the scaled spatial coordinate η; therefore the velocity and the temperature profiles in the physical space are locally distorted by the density variations.

6. The temperature distribution in the solid

In a similar way, the temperature distribution in the solid is obtained by substituting the expressions (4.2) of $\Theta_w(s)$ in equations (3.8), (3.10) and, then, performing the inverse Laplace transform. The isothermal case is complicated by the appearance of products of series. By applying the Cauchy rule we obtain

https://doi.org/10.1017/S002211200500529X Published online by Cambridge University Press

isothermal case

$$\bar{\theta}(\tau,\eta)=\theta_{w0}\left\{\operatorname{erfc}\left(\frac{1-Y}{2\sqrt{t_{\mathrm{fs}}\tau}}\right)-\operatorname{erfc}\left(\frac{1+Y}{2\sqrt{t_{\mathrm{fs}}\tau}}\right)+\sum_{n=1}^{\infty}B_n\left[\operatorname{erfc}\left(\frac{2n+1-Y}{2\sqrt{t_{\mathrm{fs}}\tau}}\right)-\operatorname{erfc}\left(\frac{2n+1+Y}{2\sqrt{t_{\mathrm{fs}}\tau}}\right)\right]\right\}+\theta_e\left\{\operatorname{erfc}\left(\frac{Y}{2\sqrt{t_{\mathrm{fs}}\tau}}\right)+\sum_{n=1}^{\infty}B_n\left[\operatorname{erfc}\left(\frac{2n+Y}{2\sqrt{t_{\mathrm{fs}}\tau}}\right)-\operatorname{erfc}\left(\frac{2n-Y}{2\sqrt{t_{\mathrm{fs}}\tau}}\right)\right]\right\},\quad(6.1a)$$

adiabatic case

$$\bar{\theta}(\tau,\eta)=\theta_{w0}\sum_{n=0}^{\infty}A^n\left[\operatorname{erfc}\left(\frac{2n+1-Y}{2\sqrt{t_{\mathrm{fs}}\tau}}\right)+\operatorname{erfc}\left(\frac{2n+1+Y}{2\sqrt{t_{\mathrm{fs}}\tau}}\right)\right],\qquad(6.1b)$$

where $A_n=\sum_{i=1}^{n}(-A)^{i-1}$ and $B_n=1-\kappa A_n$.

The time evolution of the temperature distribution in the solid is also plotted in figure 6 for both the isothermal and adiabatic cases. The figure highlights that for $\tau\to 0$ and $Y\to 1$ the temperature distributions in the solid for the isothermal and for the adiabatic case are equal: for very small time values the unwetted side of the plate is infinitely far from the solid–fluid interface and, locally, does not influence the temperature distribution.

It is interesting to note that in the isothermal case with heating ($\theta_e>0$), an example given in figure 6, the temperature distribution is not monotone for small times. This behaviour clearly cannot be represented by the linear approximation proposed by Pozzi *et al.* (1993), explaining the poor accuracy of their results for $\tau\to 0$. The temperature distribution becomes monotone when $Nu_s=0$; the corresponding time (τ_{in}) is a guess of the lower limit at which the assumption of a linear temperature distribution in the solid is valid. An approximated expression for τ_{in} is obtained by taking into account the leading terms in equation (4.5*a*):

$$\bar{\tau}_{in}\approx\left\{\ln\left[16\left(\frac{\theta_e}{\theta_{aw}}\right)^4-\frac{8\Lambda}{1+\Lambda}\right]\right\}^{-1}.\qquad(6.2)$$

By using data of figure 5(*a*) this relation provides $\bar{\tau}_{in}=0.275$, in good agreement with the result shown in the figure.

7. Conclusions

In this work a solution has been proposed for the conjugated heat transfer problem over a thick plate (infinite in both directions) that is impulsively accelerated. The *exact* energy equations have been solved in the fluid and in the solid. This solution provides an accurate analysis of the time development of the temperature field, in particular at the solid–fluid interface and of its influence on the viscous flow arising over the plate. The application of the Stewartson–Dorodnitsin transformation also makes it possible to extend the application of the results to compressible flows. Two cases were studied, defined by the condition imposed on the unwetted side of the plate (isothermal and adiabatic). The solutions, obtained analytically and explicitly by means of Laplace transform, highlight the dependence on the variables and the physical parameters governing the phenomena. Both cases are characterized by a time discontinuity of the temperature at the solid–fluid interface for very small time values.

https://doi.org/10.1017/S002211200500529X Published online by Cambridge University Press

This discontinuity is defined in terms of the adiabatic wall temperature and by the coupling parameter E_R, the ratio between the thermal effusivities in the fluid and in the solid, and it vanishes for $E_R \to 0$. For larger time values, the present solutions are in agreement with previous results relying on an approximate solution of the temperature field in the solid; nonetheless the present results suggest some limitations of the previous analysis for small time values.

E_R is the only parameter related to conjugated effects which influences the temperature and heat flux distributions if the time scale and the Nusselt number are defined by properties of the solid. In non-dimensional variables, the influence of E_R on the conjugated effects in the fluid is completely different for the isothermal and the adiabatic cases: in the isothermal case conjugated effects become negligible as $E_R \to 0$; on the contrary, they are negligible in the adiabatic case for $E_R \to \infty$.

The results given in the present paper cannot be obtained by previous analytical or numerical work. In the following we show some results obtainable through the analytical form of the solution.

7.1. *Isothermal case*

Local and asymptotic behaviour of the interface temperature and heat flux:

$\tau \to 0$:

$$\theta_w(t_{\mathrm{fs}}\tau) \approx \theta_{w0}\left[1 - \frac{\kappa}{\sqrt{\pi}}\sqrt{t_{\mathrm{fs}}\tau}\,\mathrm{e}^{-1/(t_{\mathrm{fs}}\tau)}\right] + 2\theta_e \frac{\kappa}{\sqrt{\pi}}\sqrt{t_{\mathrm{fs}}\tau}\,\mathrm{e}^{-1/(2t_{\mathrm{fs}}\tau)}, \tag{7.1}$$

$$Nu_s(t_{\mathrm{fs}}\tau) \approx \frac{\Lambda}{\sqrt{\pi}\sqrt{t_{\mathrm{fs}}\tau}}(\theta_{aw} - \theta_{w0}). \tag{7.2}$$

$\tau \to \infty$:

$$\theta_w(t_{\mathrm{fs}}\tau) \approx \theta_e + \frac{\Lambda}{\pi\sqrt{t_{\mathrm{fs}}\tau}}(\theta_{aw} - \theta_e), \tag{7.3}$$

$$Nu_s(t_{\mathrm{fs}}\tau) \approx \frac{\Lambda}{\sqrt{\pi}\sqrt{t_{\mathrm{fs}}\tau}}(\theta_{aw} - \theta_e). \tag{7.4}$$

Characteristic time necessary to reach the steady state, defined by $|\theta_w(\bar{\tau}_{st}) - \theta_e| = \epsilon$:

$$\bar{\tau}_{st} \approx \frac{\Lambda^2}{\pi^2\epsilon^2}(\theta_{aw} - \theta_e)^2. \tag{7.5}$$

7.2. *Adiabatic case*

Local and asymptotic behaviour of the interface temperature and heat flux:

$\tau \to 0$:

$$\theta_w(t_{\mathrm{fs}}\tau) \approx \theta_{w0}\left[1 + \frac{\kappa}{\sqrt{\pi}}\sqrt{t_{\mathrm{fs}}\tau}\,\mathrm{e}^{-1/(t_{\mathrm{fs}}\tau)}\right], \tag{7.6}$$

$$Nu_s(t_{\mathrm{fs}}\tau) \approx \frac{\Lambda}{\sqrt{\pi}\sqrt{t_{\mathrm{fs}}\tau}}(\theta_{aw} - \theta_{w0}). \tag{7.7}$$

$\tau \to \infty$:

$$\theta_w(t_{\mathrm{fs}}\tau) \approx \theta_{aw}\left(1 - \frac{1}{\pi\Lambda\sqrt{t_{\mathrm{fs}}\tau}}\right), \tag{7.8}$$

https://doi.org/10.1017/S002211200500529X Published online by Cambridge University Press

$$Nu_s(t_{fs}\tau) \approx \frac{\theta_{aw}}{2\sqrt{\pi}(t_{fs}\tau)^{3/2}}. \tag{7.9}$$

Characteristic time necessary to reach the steady state, defined by $|\theta_w(\bar{\tau}_{st}) - \theta_{aw}| = \epsilon$:

$$\bar{\tau}_{st} \approx \frac{\theta_{aw}^2}{\pi^2 \Lambda^2 \epsilon^2}. \tag{7.10}$$

Appendix. Asymptotic analysis of the solution

The initial and asymptotic behaviour of the temperature at the solid–fluid interface can be better identified by analysing the solution in the transformed space.

Denoting by $F(s)$ the Laplace transform of $f(t)$, the Abelian and Tauberian theorems ensure that

1. if, for $t \to 0$, $f(t) \to At^a$ then, for $s \to \infty$, $F(s) \to A\Gamma(a+1)/s^{a+1}$;
2. if, for $t \to \infty$, $f(t) \to At^a$ then, for $s \to 0$, $F(s) \to A\Gamma(a+1)/s^{a+1}$;

where $\Gamma(x)$ is the gamma function.

By theorem 1, the local behaviour of $\theta_w(\tau)$ for $\tau \to 0$ can be found by looking for the behaviour of $\Theta_w(s)$ (relations (3.13)) for $s \to \infty$ and then performing the inverse transform, again as suggested by theorem 1. Similarly, by theorem 2, the asymptotic behaviour of $\theta_w(\tau)$ for $\tau \to \infty$ can be found by looking for the behaviour of $\Theta_w(s)$ for $s \to 0$ and then performing the inverse transform. For example, the leading term of both relations (3.13) for $s \to \infty$ is $\Theta_{w0}(s) = \theta_{w0}/s$ providing $\theta_w(0) = \theta_{w0}$ in the physical space by theorem 1.

The first-order correction can be found in the same way by analysing $\Theta_w(s) - \Theta_{w0}(s)$. This procedure can be generalized to find higher-order terms; but care must be used in the expansion because no term can be a constant (the inverse transform of a constant does not exist).

The asymptotic analysis of the heat flux is also convenient in the transformed space: at the solid–fluid interface, the transformed heat flux can be expressed in terms of the transformed temperature (second equation in (3.6)).

Looking, for instance, at the behaviour of Nu_s for $\tau \to \infty$ in the adiabatic case, the first step is to identify the leading term and the first-order correction of $\Theta_w(s)$ for $s \to 0$:

$$\Theta_{w0_\infty}(s) = \frac{\theta_{aw}}{s}, \qquad \Theta_{w1_\infty}(s) = \frac{\theta_{aw}}{s}\frac{(\mathrm{e}^{-2\sigma} - 1)}{2\Lambda}. \tag{A 1}$$

Therefore, taking into account this result, the transformed heat flux is

$$\left(\frac{\partial \Theta}{\partial \eta}\right)_w (s) = \sqrt{sPr}\left[\frac{\theta_{aw}}{s} - \Theta_w(s)\right] = -\sqrt{Pr}\sqrt{s}\Theta_{w1_\infty}(s). \tag{A 2}$$

The inverse transform of this relation provides formula (7.9). The exponential in the second of equations (A 1) cannot be replaced by its local behaviour for $s \to 0$ in order to avoid the appearance of a constant term.

REFERENCES

Abramowitz, M. & Stegun, I. A. 1965 *Handbook of Mathematical Functions*. Dover.

Cole, K. D. 1997 Conjugate heat transfer from a small heated strip. *Intl J. Heat Mass Transfer* **40**, 2709–2719.

Erdélyi, A. 1954 *Tables of Integral Transforms*, vol. 2. McGraw-Hill.

Hanin, M. 1960 On Rayleigh's problem for compressible fluids. *Q. J. Mech Appl. Maths* **13**, 184–198.

https://doi.org/10.1017/S002211200500529X Published online by Cambridge University Press

Luikov, A. V. 1974 Conjugated convective heat transfer problems. *Intl J. Heat Mass Transfer* **17**, 257–265.

Luikov, A. V., Aleksashenko, V. A. & Aleksashenko, A. A. 1971 Analytical methods of solution of conjugated problems in convective heat transfer. *Intl J. Heat Mass Transfer* **14**, 1047–1056.

Moraga, N. O. & Medina, E. E. 2000 Conjugate forced convection and heat conduction with freezing of water content in a plate shaped food. *Intl J. Heat Mass Transfer* **43**, 53–67.

Niemela, J. J. & Sreenivasan, K. R. 2003 Confined turbulent convection. *J. Fluid Mech.* **481**, 355–384.

Perelman, L. T. 1961 On conjugated problems of heat transfer. *Intl J. Heat Mass Transfer* **3**, 293–303.

Pozzi, A., Bassano, E. & de Socio, L. 1993 Coupling of conduction and forced convection past an impulsively started infinite plate. *Intl J. Heat Mass Transfer* **36**, 1799–1806.

Pozzi, A. & Lupo, M. 1989 The coupling of conduction with forced convection over a flat plate. *Intl J. Heat Mass Transfer* **32**, 1207–1214.

Pozzi, A. & Tognaccini, R. 2000 Coupling of conduction and convection past an impulsively started semi-infinite flat plate. *Intl J. Heat Mass Transfer* **43**, 1121–1131.

Pozzi, A. & Tognaccini, R. 2001 Symmetrical impulsive thermo-fluid dynamic field along a thick plate. *Intl J. Heat Mass Transfer* **44**, 3281–3293.

Pozzi, A. & Tognaccini, R. 2004 On the thermal field in the impulsive Rayleigh flow. *Phys. Fluids*, **16**.

Schlichting, H. & Gersten, K. 2000 *Boundary-Layer Theory*, 8th Edn, Springer.

Tsai, S. F., Sheu, T. W. H. & Lee, S. M. 1998 Heat transfer in a conjugate heat exchanger with wavy fin surface. *Intl J. Heat Mass Transfer* **42**, 1735–1746.

Van Dyke, M. D. 1952 Impulsive motion of an infinite plate in a viscous compressible flow. *Z. Angew. Math. Phys.* **3**, 343–353.

Verzicco, R. 2002 Sidewall finite-conductivity effects in confined turbulent thermal convection. *J. Fluid Mech.* **473**, 201–210.

Verzicco, R. 2004 Effects of nonperfect thermal sources in turbulent thermal convection. *Phys. Fluids* **16**, 1965–1979.

Vynnycky, M., Kimura, s. & Kanev, K. 1998 Forced convection heat transfer from a flat plate: the conjugate problem. *Intl J. Heat Mass Transfer* **41**, 45–59.

White, F. M. 1974 *Viscous Fluid Flow*. McGraw-Hill.

https://doi.org/10.1017/S002211200500529X Published online by Cambridge University Press